Electric-Field-Induced Spin Flop in $BiFeO_3$ Single Crystals at Room Temperature

D. Lebeugle,[1] D. Colson,[1] A. Forget,[1] M. Viret,[1] A. M. Bataille,[2] and A. Gukasov[2]
[1]*Service de Physique de l'Etat Condensé, DSM/IRAMIS, CEA Saclay, F-91191 Gif-Sur-Yvette, France*
[2]*Laboratoire Leon Brillouin, DSM/IRAMIS, CEA Saclay, F-91191 Gif-Sur-Yvette, France*
(Received 24 January 2008; published 2 June 2008)

Bismuth ferrite, $BiFeO_3$, is the only known room-temperature magnetic ferroelectric material. We demonstrate here, using neutron scattering measurements in high quality single crystals, that the antiferromagnetic and ferroelectric order parameters are intimately coupled. Initially in a single ferroelectric state, our crystals have a canted antiferromagnetic structure describing a unique cycloid. Under electrical poling, polarization reorientation induces a spin flop. We argue here that the coupling between the two orders may be stronger in the bulk than in thin films where the cycloid is absent.

DOI: 10.1103/PhysRevLett.100.227602 PACS numbers: 77.80.−e, 75.50.Dd, 77.84.Bw, 78.70.Nx

Electricity and magnetism are properties which are closely linked to each other. This link is dynamic in essence, as moving charges generate a magnetic field and a changing magnetic field produces an electric field. This forms the basis of Maxwell's equations. In a solid, a similar coupling was first considered by Pierre Curie [1] between the magnetization $\vec{M}$ and electric polarization $\vec{P}$. This magnetoelectric (ME) effect was recently understood to be potentially important for applications because in information technology, it would allow magnetic information to be written electrically (with low energy consumption) and to be read magnetically. The ME effect was demonstrated and studied in the 1960s in Russia [2] and since then, many so-called ''multiferroic'' materials have been identified [3]. However, so far the magnitude and operating temperatures of any observed ME coupling have been too low for applications. In fact, the only known multiferroic material of potential practical interest is bismuth ferrite $BiFeO_3$ which is actually antiferromagnetic below $T_N \approx 370\,^{\circ}C$ [2] and ferroelectric with a Curie temperature of $\approx 820\,^{\circ}C$ [4]. As a result, in recent years, there has been a resurgence in the research conducted on this material. Moreover, epitaxial strain in $BiFeO_3$ thin films has been described as a unique way of enhancing magnetic and ferroelectric properties [5]. It is actually unclear whether this is indeed the case and in order to clarify this point, the intrinsic properties of the bulk material need to be better understood. It is surprising that although $BiFeO_3$ has been extensively studied over the past 50 years, some of its most basic properties are still not fully known. For instance, it is only in 2007 that its spontaneous polarization at room temperature has been measured to be in excess of 100 $\mu C/cm^2$ [6]. Moreover, the coupling between magnetism and ferroelectricity has only been evidenced in thin films [7] very recently. The lack of accurate data in the bulk stems from the difficulty in making high quality single crystals, a task we have recently achieved using the flux technique [6,8]. Our single crystals are usually produced in the form of platelets 40–50 microns thick and up to 3 mm^2 in area. Polarized light imaging and $P(E)$ measurements [8] indicate that the as-grown crystals are generally in a single ferroelectric and ferroelastic domain state, which may be linked to their low synthesis temperature below the ferroelectric Curie point. We report here on a neutron study of the coupling between magnetic and ferroelectric orders in two of these crystals.

Our $BiFeO_3$ single crystals are rhombohedral at room temperature with the space group $R3c$ and a pseudocubic cell with $a_{pc} = 3.9581$ Å, $\alpha_{pc} = 89.375°$ [$a_{hex} = 5.567(8)$ Å, $c_{hex} = 13.86(5)$ Å in the hexagonal setting], in perfect agreement with previous reported data [9]. No ferroelastic twinning was observed and the elongated rhombohedral direction, which is parallel to the polarization, is indexed as [111]. Fe^{3+} ions are ordered antiferromagnetically (G-type) and their moments describe a cycloid with a period of 62 nm, as established by neutron diffraction on sintered samples [10,11]. Because of the rhombohedral symmetry, there are three equivalent propagation vectors for the cycloidal rotation: $\vec{k}_1 = [\delta\, 0 - \delta]$, $\vec{k}_2 = [0\, \delta - \delta]$ and $\vec{k}_3 = [-\delta\, \delta\, 0]$ where $\delta = 0.0045$. In powder neutron diffraction, the different equally populated $\vec{k}$ domains lead to a splitting of magnetic peaks along three directions. Thus the determination of modulated magnetic ordering is not unique because elliptical cycloids and spin density waves (SDW) give the same diffraction pattern [11]. The exact nature of the periodic structure is actually an important parameter since recent models of magnetoelectric coupling give a nonvanishing electric polarization for cycloids and zero polarization for a SDW [11,12]. It is possible to eliminate this ambiguity in a single crystal by performing high-resolution scans around the strongest magnetic reflections. This is, however, a difficult experimental challenge because the long period imposes an extremely high angular resolution. The diffractometer used in this work is ''Super 6T2'' [13] in the ''Laboratoire Léon Brilloin'' in Saclay (France), where a resolution of 0.15° vertically and 0.1° horizontally can be achieved. We have measured the intensity distribution of the as-grown crystals around the four antiferromagnetic Bragg reflections of $(\frac{1}{2}, \frac{1}{2}, \frac{1}{2})$ type. The peak splitting occurs only along one of the

three symmetry allowed directions as shown for the $(\frac{1}{2}, \frac{-1}{2}, \frac{1}{2})$ reflection in Fig. 1(a). Hence, the modulated structure has a unique propagation vector $\vec{k}_1 = [\delta\, 0 - \delta]$ with $\delta = 0.004\,37$ corresponding to a period of 64 nm. The elongated shape of the measured satellites is due to the better resolution in the horizontal direction (along $[1\,0-1]$) but also possibly because of a slight warping of the sample induced by the silver epoxy electrodes apposed on both sides of the crystals for electric poling. It is in any case in complete agreement with the measured shape of the purely nuclear [111] peaks.

The spin rotation plane can also be determined because the magnetic scattering amplitude depends on the component of magnetic moments perpendicular to the scattering vector. A quantitative analysis of the integrated intensities of 10 theta/two-theta magnetic reflections (see Table I) allows us to conclude unambiguously that the moments lie in the plane defined by $\vec{k}_1 = [\delta\, 0 - \delta]$ and the polarization vector $\vec{P} \parallel [111]$ [Fig. 1(b)]. The structure refinement gives $\mu_{Fe} = 4.11(15)\mu_B$ and confirms that the periodic structure is indeed a circular cycloid with an agreement factor $R_F = 4.1\%$ and $\chi^2 = 1.52$. Using a SDW model, or introducing a 20% ellipticity, deteriorates significantly the fit ($R_F = 19\%$ and $\chi^2 = 9.2$). A consequence of the single $\vec{k}$ vector of the cycloid is that the crystal symmetry is lowered. Indeed, the ternary axis is lost and the average symmetry becomes monoclinic with the principal direction along $\vec{k} = [1\,0-1]$ [14].

No electric field effect on the magnetic order has ever been reported in bulk $BiFeO_3$. Here, we analyze the effect of poling in the [010] direction perpendicular to the plate-let. As the first coercive field is reached, a significant decrease in the $(\frac{1}{2}, \frac{-1}{2}, \frac{1}{2})$ neutron reflection intensity is observed, indicating a redistribution of the average rhombohedral distortion. After reaching a multidomain state with $\langle P \rangle \approx 0$, several neutron diffraction scans were performed and we found that the vertical resolution used for the virgin state (in Fig. 1) was not sufficient. Indeed, because ferroelastic twins complicate the diffraction patterns, we had to reach a resolution of 0.1° in both horizontal and vertical directions to obtain a meaningful measurement. This pushes the experimental conditions to the limit of what can be done with these instruments. Figure 2(b) shows the (3D) reciprocal space mapping of the crystal. Yellow (or light gray) (111) type reflections are purely nuclear in origin while the red (or gray) $(\frac{1}{2}, \frac{1}{2}, \frac{1}{2})$ are purely magnetic. (111) and (1 −11) reflections are split along the long diagonals (dashed lines), which indicates the presence of two domains with different interplane distances. These are two rhombohedral twins with polarization axes along [111] and $[1-11]$, 45%–55% in volume. The other (−111) and (11 −1) reflections are also split, but along the [101] direction. This is due to a buckling of the crystal schematically shown in Fig. 2(a), which slightly changes the angles fulfilling the Bragg conditions. This is fully consistent with polarized optical microscope images taken on similar crystals [Fig. 2(a)] indicating that the multidomain state consists of stripe regions with two different polarization directions.

The purely antiferromagnetic peaks have been analyzed in more detail. The strongest $(\frac{1}{2}, \frac{-1}{2}, \frac{1}{2})$ reflection is shown in the zoomed region of Fig. 2(b) to be composed of four spots. These result from two simultaneous splits, one due to the ferroelectric distortion (already evidenced in the nuclear peaks) and one of magnetic origin. A projection of the zoomed area is represented in Fig. 3 on which green spots indicate the expected reflections from $\vec{P}_{111}$ (lower

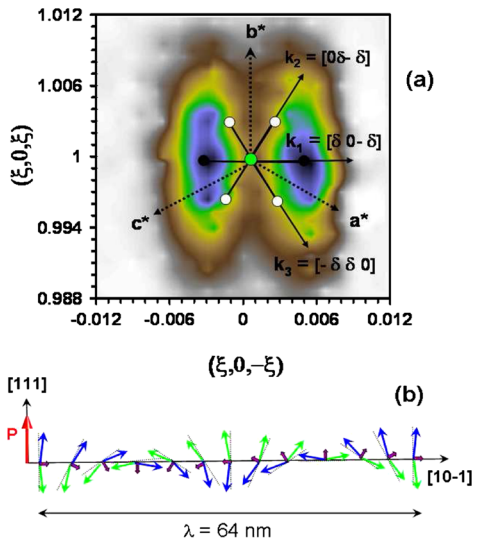

FIG. 1 (color online). (a) Neutron intensity around the $(\frac{1}{2}, \frac{-1}{2}, \frac{1}{2})$ Bragg reflection in the virgin, single domain, state. The two diffraction satellites indicate that the cycloid is along the $[1\,0\,-1]$ direction. (b) Schematics of the 64 nm antiferromagnetic circular cycloid.

TABLE I. Intensity measured around the magnetic Bragg positions compared to that expected for a cycloid with magnetic vectors in the different allowed $(\vec{P}, \vec{k})$ planes. $R_F = 4.1\%$ and $\chi^2 = 1.52$ (the relevant intensities are in boldface).

Bragg peak	$\vec{P}, \vec{k}_1$	$\vec{P}, \vec{k}_2$	$\vec{P}, \vec{k}_3$	I_{obs}
$\frac{1}{2}, \frac{-1}{2}, \frac{1}{2}$	**189**	122	122	**198(8)**
$(\frac{1}{2}, \frac{1}{2}, \frac{1}{2})$	**100**	100	100	**99(6)**
$(\frac{-1}{2}, \frac{1}{2}, \frac{1}{2})$	**122**	122	189	**116(6)**
$(\frac{1}{2}, \frac{1}{2}, \frac{-1}{2})$	**122**	189	122	**114(6)**
$(\frac{1}{2}, \frac{-3}{2}, \frac{1}{2})$	**113**	71	71	**111(11)**
$(\frac{3}{2}, \frac{-1}{2}, \frac{-1}{2})$	**71**	71	113	**83(8)**
$(\frac{-1}{2}, \frac{-1}{2}, \frac{3}{2})$	**71**	113	71	**83(8)**
$(\frac{-1}{2}, \frac{-3}{2}, \frac{-1}{2})$	**71**	61	61	**78(9)**
$(\frac{3}{2}, \frac{1}{2}, \frac{1}{2})$	**61**	61	71	**52(6)**
$(\frac{1}{2}, \frac{1}{2}, \frac{1}{2})$	**61**	71	61	**56(7)**

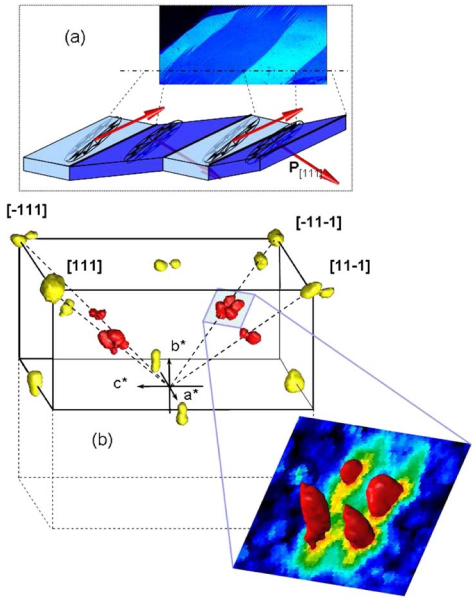

FIG. 2 (color online). Mapping of the neutron intensity in reciprocal space. Two sets of splitting appear for the nuclear intensity (yellow or light gray spots) due to the presence of two ferroelastic domains [see (a)]: one because of the presence of two rhombohedral distortions along [111] and $[1\,{-}11]$, and the second because of a physical buckling of the crystal induced by the twinning. Magnetic peaks are further split because of the cycloids. Note that because the splitting is small, the scale has been magnified by a factor of 10 around each peak position.

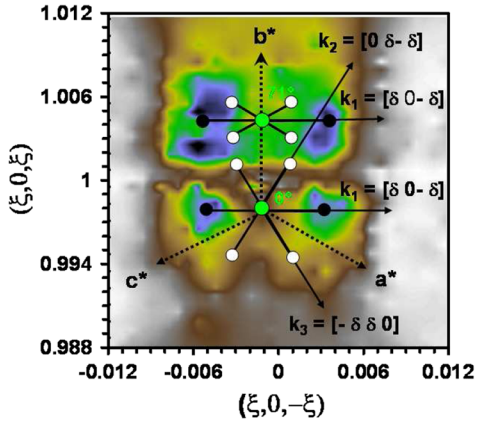

FIG. 3 (color online). Neutron intensity around the $(\frac{1}{2}, \frac{-1}{2}, \frac{1}{2})$ Bragg position in the multidomain state. Theoretical positions are indicated by the black and white spots. Diffraction satellites are visible in the 0° (bottom half) and 71° (top half) domains of polarization. The difference in vertical spot shape likely originates from the position of reversed domains at opposite ends of the sample because of a preferred nucleation near the edges. Any warping of the sample splits the new $(1\,{-}11)$ peak while recovering an improved resolution for the original domain located near the center.

half of the pattern) and $\vec{P}_{1-11}$ (upper half) domains. The magnetic satellites are also indicated as black spots for the cycloid in the original $[-1\,0\,1]$ direction and white spots for the other two symmetry allowed ones. In the $\vec{P}_{1-11}$ domains (where the polarization rotated by 71° under poling) the expected satellites are not in a regular rhombohedral symmetry because they correspond to a projection on the (111) diffraction plane of the figure, from which they do not belong. In the data of Fig. 3, the splitting is only in the horizontal direction for both domains indicating that the $[\delta\,0\,{-}\delta]$ propagation vector of the cycloid remains the same as that in the virgin state. Importantly, because the applied electric field is along [010], the virgin state can never be recovered because a single [111] type of electric domain cannot be fully repopulated.

The rotation planes of the AF vectors in the two domains can again be determined using the integrated intensities of the magnetic reflections (Table II). These can be well accounted for by considering that 55% of the crystal volume has switched its polarization by 71°, and brought with it the rotation plane of the Fe moments, thus inducing a spin flop of the antiferromagnetic sublattice. In each domain, AF moments make a cycloid by rotating in the plane defined by $\vec{k}_1$ and $\vec{P}$ as represented in Fig. 4. This unambiguously demonstrates that the magnetic Fe^{3+} structure is intimately linked to the polarization vector. This negates the common belief that in bulk $BiFeO_3$ the magnetoelectric coupling must be weak because the cycloid cancels linear ME effects [15–18]. Although $\langle M \rangle = 0$ imposes a zero global linear ME effect, the coupling between $\vec{M}$ and $\vec{P}$ at the atomic level still exists. The underlying relevant mechanism is the (generalized) Dzyaloshinskii-Moriya (DM) [19] interaction which has recently been readdressed starting from electronic Hamiltonians including spin-orbit coupling [20,21]. Katsura *et al.* [20] describe in terms of spin currents the polarization induced by a cycloidal spin arrangement, which can be written as $\vec{P} \propto \vec{e}_{ij} \times (\vec{S}_i \times \vec{S}_j)$, with $\vec{S}_{i,j}$ the local spins and $\vec{e}_{ij}$ the unit vector connecting the two sites. The interaction of this polarization with a coexisting internal polarization produces a magnetoelectric term in the total energy [20]: $E_{\mathrm{DM}} = (\vec{P} \times \vec{e}_{ij}) \cdot (\vec{S}_i \times \vec{S}_j)$. This ME interaction, which can also be obtained

TABLE II. Intensity measured around the magnetic Bragg positions compared to that expected for a cycloid with magnetic vectors in the different allowed planes. Calculated values are obtained with 55% of domains having switched their polarization by 71° and kept the same propagation vector. $R_F = 4.9\%$ and $\chi^2 = 1.9$ (the relevant intensities are in boldface).

Bragg peak	$\vec{P}_0, \vec{k}_1$	$\vec{P}_{71}, \vec{k}'_1$	$\vec{P}_{71}, \vec{k}'_2$	$\vec{P}_{71}, \vec{k}'_3$	I_{obs}	I_{calc}
$(\frac{1}{2}, \frac{-1}{2}, \frac{1}{2})$	**189**	**100**	100	100	**158(7)**	**150**
$(\frac{1}{2}, \frac{1}{2}, \frac{1}{2})$	**100**	**189**	122	122	**145(6)**	**139**
$(\frac{-1}{2}, \frac{1}{2}, \frac{1}{2})$	**122**	**122**	122	189	**120(8)**	**122**
$(\frac{1}{2}, \frac{1}{2}, \frac{-1}{2})$	**122**	**122**	189	122	**112(9)**	**122**

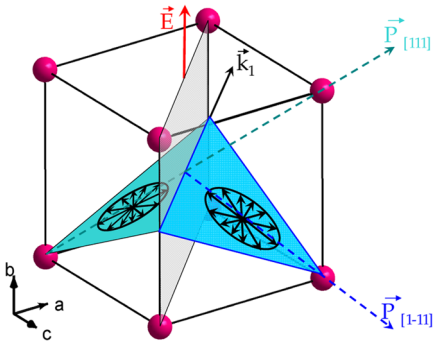

FIG. 4 (color online). Schematics of the planes of spin rotations and cycloids $\vec{k}_1$ vector for the two polarization domains separated by a domain wall (in light gray).

from symmetry considerations [12,18], was held responsible for the cycloidal spin arrangement in $BiFeO_3$ [18]. This coupling energy induces the canting of Fe moments which exactly compensates for the loss in exchange energy (neglecting anisotropy): $E = -Ak^2$. A ME energy density of -3×10^7 J/m^3 can be inferred from the value of the period of the cycloid and the exchange constant ($A = 3 \times 10^{-6}$ J/m). Importantly, the coupling energy is zero when $\vec{P}$ is perpendicular to the local moments and maximum when it lies in the cycloid rotation plane. This explains the antiferromagnetic flop we observe when $\vec{P}$ changes direction. This also explains why the two crystals we measured had their cycloids along the same direction $\vec{k}_1$. Indeed, this minimizes the components of the magnetic spins parallel to the depolarization field (normal to the platelets surface), which lowers the cost in DM energy.

When in thin film form, $BiFeO_3$ is a very different system because epitaxial strain suppresses the cycloid and induces a weak magnetic moment [22]. Locally, the magnetic structure consists of canted spins with angles alternating sign between neighboring unit cells, which makes the moments add. If this magnetic configuration were to generate a local polarization, its direction would alternate from site to site. Therefore, in order for a global polarization to coexist with weak ferromagnetism, it is more favorable if the spins lie in a plane perpendicular to the polarization direction, a configuration for which the DM based interactions are zero. This is exactly what is observed in $BiFeO_3$ films [5]. The magnitude of this ME coupling is more difficult to estimate than that in the bulk, but because it originates from the frustration of the DM interactions, it is likely to be weaker. Interestingly, canting angles are only about 0.2° (the weak ferromagnetic moment being $0.02\mu_B$/atom [22]), to be compared with the 2.25° imposed by the cycloid in the bulk. This underlines the ME origin of the cycloid and also hints at a stronger coupling in the bulk since the interaction between $\vec{P}$ and $\vec{M}$ is directly linked to the angles between neighboring spins.

In order to make a useful device with $BiFeO_3$, we suggest using the exchange bias interaction between a thin ferromagnetic layer and a $BiFeO_3$ substrate. It should be possible to vary electrically the exchange bias interaction using the antiferromagnetic flop observed here. Indeed, in conventional exchange bias systems, a noncompensated antiferromagnetic surface is not a prerequisite to obtain a large exchange field. Hence, it is likely that the cycloid may not significantly affect the bias, while optimizing the coupling between the antiferromagnetic and ferroelectric orders.

We would like to acknowledge fruitful discussions with Frederic Ott, Hans Schmid, Alexander Zhdanov, and Daniel Khomskii as well as funding from the "Agence Nationale de la Recherche" through Contract No. NT05-1-45147 "FEMMES." We also thank X. Le Goff for x-ray measurements as well as Gustau Catalan, Neil Mathur, and Manuel Bibès for their critical reading of the manuscript.

[1] P. Curie, J. Phys. **3**, 393 (1894).
[2] G. Smolenskii and I. Chupis, Sov. Phys. Usp. **25**, 475 (1982); Y. Venevtsev and V. Gagulin, Ferroelectrics **162**, 23 (1994), and references therein.
[3] M. Fiebig, J. Phys. D **38**, R123 (2005); W. Eerenstein, N. D. Mathur, and J. F. Scott, Nature (London) **442**, 759 (2006).
[4] R. Smith *et al.*, J. Appl. Phys. **39**, 70 (1968).
[5] J. Wang *et al.*, Science **299**, 1719 (2003).
[6] D. Lebeugle *et al.*, Appl. Phys. Lett. **91**, 022907 (2007); V. V. Shvartsman *et al.*, Appl. Phys. Lett. **90**, 172115 (2007).
[7] T. Zhao *et al.*, Nat. Mater. **5**, 823 (2006).
[8] D. Lebeugle *et al.*, Phys. Rev. B **76**, 024116 (2007).
[9] F. Kubel and H. Schmid, Acta Crystallogr. Sect. B **46**, 698 (1990).
[10] I. Sosnowska, T. Peterlin-Neumaier, and E. Steichele, J. Phys. C **15**, 4835 (1982).
[11] R. Przenioslo, M. Regulski, and I. Sosnowska, J. Phys. Soc. Jpn. **75**, 084718 (2006).
[12] M. Mostovoy, Phys. Rev. Lett. **96**, 067601 (2006).
[13] A. Gukasov, Physica (Amsterdam) **397B**, 131 (2007).
[14] H. Schmid (private communication).
[15] C. Tabares-Munoz *et al.*, Jpn. J. Appl. Phys. **24**, 1051 (1985).
[16] Y. F. Popov *et al.*, JETP Lett. **57**, 69 (1993).
[17] J. Scott and D. Tilley, Ferroelectrics **161**, 235 (1994).
[18] A. Kadomtseva *et al.*, JETP Lett. **79**, 571 (2004).
[19] I. Dzyaloshinskii, Sov. Phys. JETP **10**, 628 (1959); T. Moriya, Phys. Rev. **120**, 91 (1960).
[20] H. Katsura, N. Nagaosa, and A. V. Balatsky, Phys. Rev. Lett. **95**, 057205 (2005).
[21] I. Sergienko and E. Dagotto, Phys. Rev. B **73**, 094434 (2006).
[22] H. Bea *et al.*, Appl. Phys. Lett. **87**, 072508 (2005); H. Bea *et al.*, Philos. Mag. Lett. **87**, 165 (2007).